Please cite this article in press as: Marangoni et al., The Transcription Factor NFAT Exhibits Signal Memory during Serial T Cell Interactions with Antigen-Presenting Cells, Immunity (2013), http://dx.doi.org/10.1016/j.immunu.2012.09.012

Immunity
Article

The Transcription Factor NFAT Exhibits Signal Memory during Serial T Cell Interactions with Antigen-Presenting Cells

Francesco Marangoni,[1,2] Thomas T. Murooka,[1,2] Teresa Manzo,[1,3] Edward Y. Kim,[1,2] Esteban Carrizosa,[1,2] Natalie M. Elpek,[1] and Thorsten R. Mempel[1,2,*]
[1]The Center for Immunology and Inflammatory Diseases (CIID), Massachusetts General Hospital, Boston, MA 02114, USA
[2]Harvard Medical School, Boston, MA 02115, USA
[3]Present address: Vita-Salute San Raffaele University, 20132 Milano, Italy
*Correspondence: tmempel@mgh.harvard.edu
http://dx.doi.org/10.1016/j.immuni.2012.09.012

SUMMARY

Interactions with antigen-presenting cells (APCs) interrupt T cell migration through tissues and trigger signaling pathways that converge on the activation of transcriptional regulators, including nuclear factor of activated T cells (NFAT), which control T cell function and differentiation. Both stable and unstable modes of cognate T cell-APC interactions have been observed in vivo, but the functional significance of unstable, serial contacts has remained unclear. Here we used multiphoton intravital microscopy in lymph nodes and tumors to show that while NFAT nuclear import was fast ($t_{1/2\ max}$~1 min), nuclear export was slow ($t_{1/2}$~20 min) in T cells. During delayed export, nuclear NFAT constituted a short-term imprint of transient TCR signals and remained transcriptionally active for the T cell tolerance gene *Egr2*, but not for the effector gene *Ifng*, which required continuous TCR triggering for expression. This provides a potential mechanistic basis for the observation that a predominance of unstable APC interactions correlates with the induction of T cell tolerance.

INTRODUCTION

The cells of the innate and adaptive immune system are dispersed throughout the body but need to communicate with each other in order to integrate their individual functions and achieve immunity against foreign but tolerance toward self antigens (Ag). This communication is facilitated through coordinated cell trafficking, which in the case of T cells enables interactions with appropriate Ag presenting cells (APCs) in both lymphoid and nonlymphoid tissues (Germain et al., 2008; Pittet and Mempel, 2008). Cognate interactions with APCs allow for the transient activation of a variety of signaling pathways in T cells through the T cell receptor (TCR) and other cell surface receptors and thus control both immediate cellular responses, such as cytokine secretion, as well as changes in gene expression that shape cellular differentiation, proliferation, and survival. A central event in T cell activation is sustained elevation of cytosolic Ca^{2+} concentration. An initial IP_3-mediated release of Ca^{2+} from the endoplasmic reticulum triggers influx of extracellular Ca^{2+} through store-operated Ca^{2+}-channels in the plasma membrane. The Ca^{2+} and calmodulin-dependent activity of calcineurin then leads to dephosphorylation and nuclear accumulation of nuclear factor of activated T cells (NFAT) transcription factors. There, NFAT proteins cooperate directly and indirectly with many other nuclear factors to control various genetic programs of T cell function (Macian, 2005).

It has long been assumed that stable, long-lasting contacts with dendritic cells (DCs) are required to trigger effector cell differentiation in naive T cells, but in situ imaging studies in explanted tissues and by multiphoton intravital microscopy (MP-IVM) reveal that both $CD4^+$ and $CD8^+$ T cells also engage in unstable and transient interactions during the initial and late stages of antigenic priming (Celli et al., 2005; Henrickson et al., 2008; Mempel et al., 2004; Miller et al., 2004). Predominantly unstable T cell contacts are observed in lymph nodes (LNs) when DCs present low-affinity TCR ligands (Skokos et al., 2007) or under conditions of T regulatory (Treg) cell-induced tolerance (Tadokoro et al., 2006; Tang et al., 2006). Tolerant $CD4^+$ T cells are also less capable of stabilizing interactions with APCs in peripheral tissues (Fife et al., 2009) and similarly, encounters of $CD8^+$ T cells with APCs in tumor tissue result in heterogeneous contact stability (Boissonnas et al., 2007; Mrass et al., 2006). In some of these imaging studies, correlative population analyses suggest that not only stable, but also unstable T cell-APC contacts are productive. However, it remains unresolved what the requirements are, in terms of duration and stability, for individual cell-cell contacts to be functionally relevant.

Here we used an approach to monitor NFAT nucleocytoplasmic shuttling in T cells by MP-IVM in murine LNs and tumor tissue in order to obtain an unambiguous read-out for productive TCR signaling in individual cells and to study how efficiently this gene regulatory pathway is activated through unstable and transient APC contacts compared to stable and longer-lasting contacts in vivo. We found that in Ag-experienced $CD8^+$ T cells, both transient and sustained contacts with different types of APCs result in near-instantaneous accumulation of NFAT in the nucleus in a seemingly binary fashion. In contrast, nuclear export upon loss of APC contact was much slower, which permitted

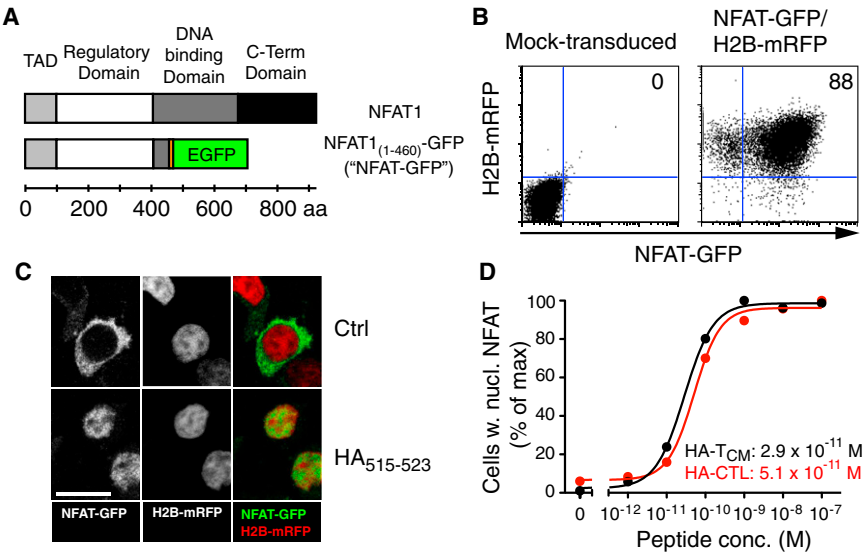

Figure 1. NFAT-GFP Nuclear Translocation Is a Sensitive Readout of TCR Triggering

(A) Domain structure of full-length murine NFAT1 and NFAT-GFP. TAD, N-terminal transactivation domain. The 6-aa linker (DPPVAT) is shown in orange.

(B) Frequency of HA-CTL expressing both NFAT-GFP and H2B-mRFP after transduction and selection. Similar results were obtained for HA-T_{CM}.

(C) HA-CTL expressing NFAT-GFP (green) and H2B-mRFP (red) were cocultured with B cells pulsed with 10 μM HA peptide or not (Ctrl). Scale bar represents 10 μm.

(D) Percentage of HA-CTL (red symbols) and HA-T_{CM} (black symbols) with visually scored nuclear NFAT upon exposure to B cells pulsed with a range of peptide doses. Each data point represents ≥100 cells. Lines are sigmoid curve-fits. Numbers are EC_{50} values. One experiment representative of two is shown.

continued transcription of the tolerance-associated NFAT target gene *Egr2*, but not of *Ifng*, during this transient period of "NFAT memory" after interruption of TCR signals. Finally, we found that Treg cell-mediated tumor tolerance was characterized by decreased stability of cytotoxic T lymphocyte (CTL)-APC interactions in tumor tissue accompanied by more widespread NFAT activation in motile cells. The resulting shift in the balance between NFAT activity during direct APC contact and during NFAT memory may result in the preferential induction of tolerogenic gene expression programs in T cells.

RESULTS

NFAT Nuclear Translocation Is a Sensitive Read-Out for TCR Signaling

The fluorescent reporter $NFAT1_{(1-460)}$-GFP ("NFAT-GFP") (Aramburu et al., 1999) is a fusion of enhanced green fluorescent protein (EGFP) with a truncated murine NFAT1 (NFATc2) that lacks the C terminus and most of the DNA-binding domain but incorporates the regulatory domain, which governs nucleocytoplasmic shuttling in NFAT 1 to 4 (Figure 1A). To test how sensitively nuclear translocation of NFAT-GFP reports TCR signaling in primary T cells, we cultured influenza hemagglutinin (HA)-specific CL4 TCR transgenic T cells under conditions producing either central memory-like ("HA-T_{CM}") or cytotoxic effector-like ("HA-CTL") $CD8^+$ T cells (see Figure S1 available online). These were retrovirally transduced to express NFAT-GFP together with monomeric red fluorescent protein-fused histone protein H2B (H2B-mRFP) as a constitutive nuclear label (Figures 1B and 1C). Expression of these reporter genes did not interfere with the expansion, differentiation, and cytokine secretion of either HA-T_{CM} or HA-CTL (Figure S1) and therefore did not measurably affect TCR signal transduction or NFAT-dependent gene expression. Conjugate formation with $HA_{515–523}$-pulsed B cells in vitro induced maximal translocation of dormant cytosolic NFAT-GFP into the nucleus of HA-CTL (Figure 1C) or HA-T_{CM} (data not shown) within less than 10 min. NFAT activation occurred in some cells at very low doses of Ag (EC_{50}: 30–50 pM) and in nearly all cells at a peptide concentration of 1 nM (Figure 1D). Thus, visualization of NFAT-GFP nucleocytoplasmic shuttling in T cells provides a highly sensitive measure of TCR stimulation.

Rapid Activation and Slow Deactivation of NFAT In Vivo

In tissues, T cells are exposed to a multitude of environmental cues, such as chemokines, which may compete with TCR signals (Bromley et al., 2000) and thus affect NFAT activation during interactions with APCs. To examine the dynamics and efficiency of NFAT activation in Ag-experienced T cells upon encounter with APCs that deliver a strong TCR as well as costimulatory signals in vivo, we seeded mice with NFAT-GFP-expressing HA-T_{CM}, prepared inflamed, tumor-draining popliteal LNs for MP-IVM analysis (Mempel et al., 2004), and recorded the initial T cell encounters with intravenously infused follicular B cells presenting the cognate HA-peptide upon their recruitment to LNs (Figure 2A). T cell contacts with peptide-pulsed B cells triggered the efficient formation of stable yet motile conjugates as described (Mempel et al., 2006; Okada et al., 2005). Immediately following contact formation, NFAT-GFP began to enter the nucleus and reached maximal cytoplasmic depletion and nuclear accumulation within as little as 2 min (Figures 2B and 2C; Movies S1 and S2). In stark contrast to these fast activation kinetics, NFAT-GFP remained nuclear for considerable periods of time after eventual interruption of cell contacts, even when T cells had already resumed motility (Figure 2D; Movie S2). Equivalent observations were made in LNs inflamed though footpad injection of tumor necrosis factor (data not shown).

An approach was developed to quantify the spatial overlap of NFAT-GFP with H2B-mRFP at varying ratios of cytoplasmic and nuclear NFAT-GFP. Lack of overlap indicated cytoplasmic localization of NFAT-GFP and was defined as an NFAT signaling index (SI) of 0, whereas full overlap indicated nuclear localization and was defined as an NFAT SI of 1 (Figure S2). This index was measured through a manually guided but automated and unbiased image analysis algorithm. Plotting the NFAT SI of HA-T_{CM} against the distance to the most proximal B cell as a function

Please cite this article in press as: Marangoni et al., The Transcription Factor NFAT Exhibits Signal Memory during Serial T Cell Interactions with Antigen-Presenting Cells, Immunity (2013), http://dx.doi.org/10.1016/j.immuni.2012.09.012

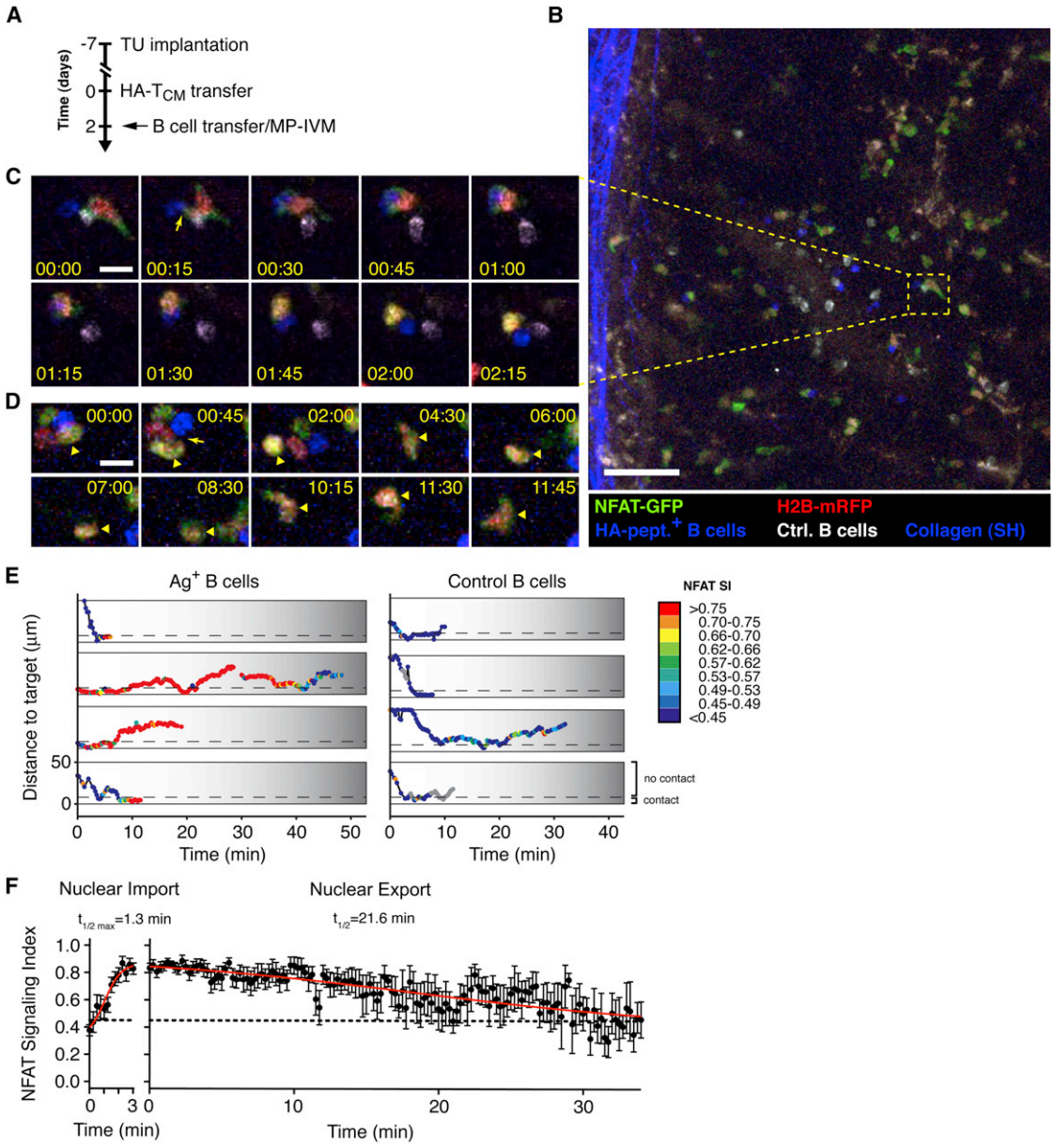

Figure 2. Kinetics of NFAT Nucleocytoplasmic Shuttling in T Cells In Vivo

(A) Experimental setup: HA-T_{CM} expressing NFAT-GFP (green) and H2B-mRFP (red) were transferred i.v. into mice with 7-day-old CT26 tumors implanted in the dorsal foot in order to maximize T_{CM} recruitment to the draining popliteal LN. Two days later, target B cells pulsed with HA-peptide (blue) or not (white) were injected i.v., and MP-IVM was started immediately.

(B) Intravital micrograph depicting a typical LN preparation. Collagen visualized through second harmonic generation (blue) outlines the LN capsule on the left. Scale bar represents 50 μm. See also Movie S1.

(C and D) Enlarged image sequences from the same (C) and a similar recording (D) as in (B), showing NFAT localization in HA-T_{CM} upon contact (arrow) with HA peptide-pulsed B cells (C) and upon interruption (arrow) of contact (D). Arrowheads in (D) identify disengaged T_{CM}. See also Movie S2. Time in min:sec. Scale bar represents 10 μm.

(E) Representative traces of HA-T_{CM} depicting the color-coded NFAT SI and the distance (between cell centroids) to the nearest HA peptide-pulsed (Ag^+) or control B cell. Dashed lines indicate 8 μm of distance, at which physical contact was typically observed. Grey symbols represent ambiguous measurements when the recorded T_{CM} made contact with both control and HA-peptide-pulsed B cells. Traces selected from 581 recorded in seven movies from two independent experiments.

(F) NFAT kinetics in vivo. For nuclear import, t = 0 represents the time of initial contact with an Ag^+ B cell (11 tracks). For nuclear export, t = 0 represents the time of detachment from an Ag^+ B cell (18 tracks at t = 0). Mean ± SEM of NFAT signaling indices are shown. Red lines are sigmoid curve-fits; $t_{1/2\ max}$: mean time to half-maximal response.

Please cite this article in press as: Marangoni et al., The Transcription Factor NFAT Exhibits Signal Memory during Serial T Cell Interactions with Antigen-Presenting Cells, Immunity (2013), http://dx.doi.org/10.1016/j.immuni.2012.09.012

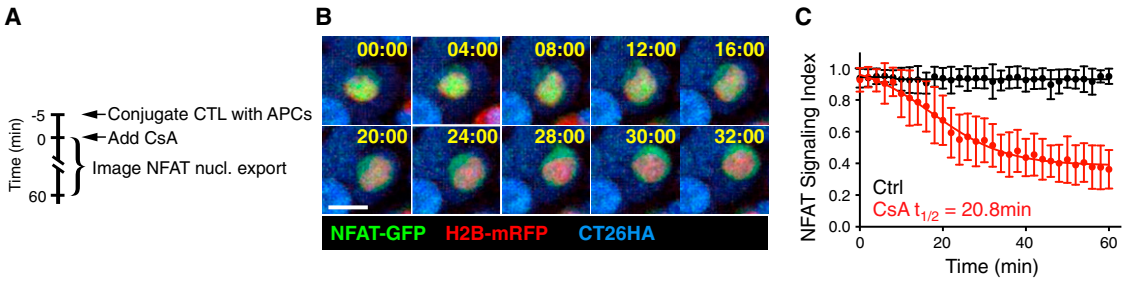

Figure 3. NFAT Nuclear Export after Calcineurin Blockade In Vitro

(A) Experimental design.

(B) Image sequence of an HA-CTL expressing NFAT-GFP (green) and H2B-mRFP (red) conjugated to CT26HA tumor cells (expressing H2B-Cerulean, blue) after addition of CsA. See also Movie S3. Time in min:sec. Scale bar represents 10 μM.

(C) Average NFAT signaling indices over time, in presence (red symbols) or absence (black symbols) of CsA. Error bars represent SD. Lines show sigmoid curve-fits. One experiment representative of two is shown.

of time confirmed that physical contacts with HA peptide-pulsed, but not control B cells, induced very rapid and sustained NFAT-GFP nuclear accumulation (Figure 2E). By averaging the import and export kinetics of many cells, we determined that NFAT activation was maximal within less than 3 min ($t_{1/2\ max}$ ~1 min) and thus only minimally delayed relative to the kinetics of cytosolic Ca^{2+} influx observed in vitro (Negulescu et al., 1996). NFAT deactivation, as reflected by a gradual return to a baseline NFAT SI, proceeded much more slowly with a half-life of about 20 min (Figure 2F).

Delayed NFAT-GFP and NFAT1 Nuclear Export Is Independent of Continued Calcineurin Activity

One potential explanation for prolonged NFAT nuclear localization after interruption of T cell-APC contacts is ongoing TCR signaling due to the transfer of cognate peptide-major histocompatibility complex (pMHC)-containing membrane from B cells to T cells through processes such as trogocytosis (Stinchcombe et al., 2001) or transendocytosis (Qureshi et al., 2011). However, when we used cyclosporine A (CsA) to pharmacologically inhibit the Ca^{2+}-dependent, NFAT-activating phosphatase calcineurin in either APC-conjugated or ionomycin-treated primary T cells, we observed similarly slow export kinetics (Figures 3A–3C, Figures S3A–S3D; Movie S3). Furthermore, to examine whether slow nuclear export of NFAT was paralleled by an equally slow decrease of intracellular Ca^{2+}, which would suggest continued TCR signaling, we activated HA-CTL with the lectin Concanavalin A (ConA) that crosslinks various cell surface receptors including the TCR but can be antagonized with the carbohydrate α-methyl mannoside (α-MM) (Das et al., 2009). Under these conditions, $[Ca^{2+}]_i$ declined with a $t_{1/2}$ of less than 3 min, whereas the $t_{1/2}$ of nuclear NFAT was 14 min (Figure S3E). Thus, transient persistence of NFAT in the nucleus reflects the rate of nuclear export upon interruption of NFAT dephosphorylation, and not waning TCR signals or gradually declining but ongoing calcineurin activity upon cessation of TCR signaling.

To determine the relative contributions of various export kinases to NFAT inactivation (Müller and Rao, 2010), we pretreated HA-CTL with chemical inhibitors and found that all three known classes of NFAT kinases were involved but that casein kinase 1 appeared to play a dominant role (Figures S3F and S3G).

We considered that due to the lack of the DNA-binding domain, NFAT-GFP measurements might underestimate the export kinetics of full-length NFAT proteins, which could be even slower due to retention through direct NFAT-DNA interactions. However, when we used antibodies to stain the N-terminal domain of both NFAT-GFP and endogenous NFAT1 in ionomycin-activated T cells treated with CsA, NFAT-GFP and total NFAT1 colocalized at all times (Figures S3B–S3D). Therefore, the export kinetics of native NFAT1 are not, or are only minimally, sensitive to DNA retention effects and closely match those of NFAT-GFP.

NFAT Is Transcriptionally Active during Delayed Nuclear Export

Previous studies have shown that T cell expression of effector cytokines is very tightly correlated with antigenic stimulation (Slifka et al., 1999). On the other hand, different mechanisms of signal memory of various duration have been described in lymphoid cells, such as a SOS-dependent metastable pool of Ras-GTP (Das et al., 2009) or expression of early response genes, such as c-*fos* (Clark et al., 2011). Based on our observation of delayed nuclear export after termination of APC contact, and on previous work that suggested NFAT memory function during Ca^{2+}-oscillations in a fibroblast cell line (Tomida et al., 2003), we hypothesized that NFAT may contribute to a short-term biochemical imprint of recent cognate interactions that enables T cells to maintain gene expression between serial contacts. We therefore sought to test whether nuclear NFAT continues to facilitate gene transcription after its activating stimulus is removed. To this end, we first stimulated HA-CTL with the protein kinase C (PKC) activator phorbol 12-myristate 13-acetate (PMA) and the Ca^{2+} ionophore ionomycin for 30 min ("priming") and then measured IFN-γ-expression immediately following this priming phase under various conditions of ongoing stimulation in the presence of brefeldin A ("measurement," Figure 4A). When actinomycin D (ActD) was added at the beginning of the measurement phase to block DNA transcription, we observed a low amount of residual IFN-γ-expression, which likely resulted from translation of transcripts generated during priming. Consequently, when messenger RNA (mRNA) translation was inhibited instead, this background gene expression during measurement disappeared. To establish

Please cite this article in press as: Marangoni et al., The Transcription Factor NFAT Exhibits Signal Memory during Serial T Cell Interactions with Antigen-Presenting Cells, Immunity (2013), http://dx.doi.org/10.1016/j.immuni.2012.09.012

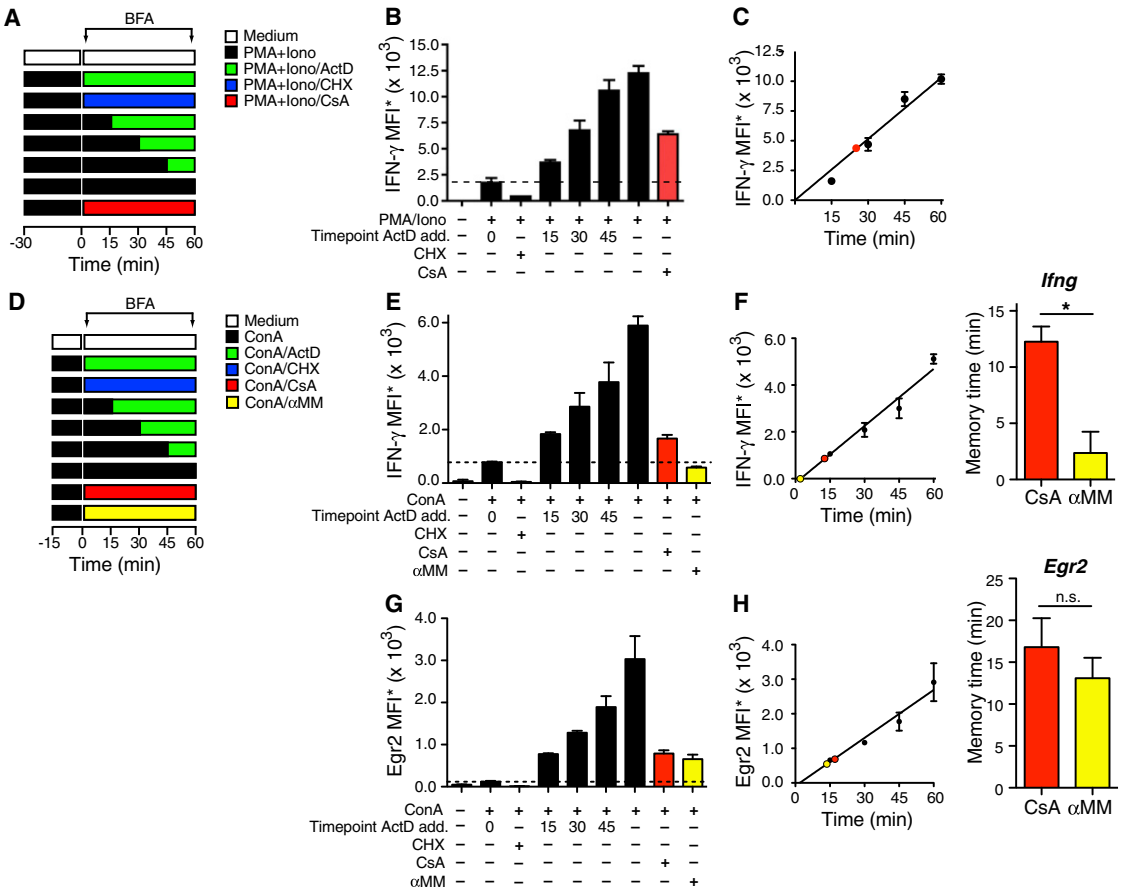

Figure 4. NFAT Is Transcriptionally Active during Nuclear Export and Promotes *Egr2*, but Not *Ifng* Expression

(A) Experimental design to measure NFAT-dependent transcription after PMA and ionomycin stimulation and calcineurin inactivation. BFA, brefeldin A; ActD, actinomycin D; CHX, cycloheximide.

(B) Intracellular IFN-γ in CTL treated with CHX, CsA, or with ActD starting at different time points during the measurement phase. Dashed line indicates background expression after addition of ActD at time 0. Mean ± SD of triplicates is shown.

(C) NFAT memory time is derived by relating expression above background of IFN-γ after CsA (red symbol) to expression during various time intervals of stimulation in absence of CsA, as shown in (B).

(D) Experimental design to measure NFAT-dependent transcription of IFN-γ and Egr2 after blockade of TCR triggering. ConA, concanavalin A; αMM, α-methyl mannoside.

(E) Intracellular IFN-γ after treatment with CHX, CsA, αMM, or with ActD starting at different time points during the measurement phase.

(F) Quantification of NFAT memory time for *Ifng* based on expression above background as shown in (E).

(G and H) Intracellular Egr2 and NFAT memory time for *Egr2* in the same experimental setting as shown for IFN-γ in (E) and (F). MFI* is the product of percentage and MFI of IFN-γ or Egr2 in cells. Mean and SD of triplicates from one representative experiment out of three is shown in (B), (C), (E), and (F). P value is derived through Student's t test. n.s., not significant; *, $p < 0.05$.

a reference curve for the amount of IFN-γ expressed per unit time, we allowed transcription to proceed for various time intervals of measurement before addition of ActD and observed a proportional, approximately linear increase in IFN-γ-expression above background. Finally, when transcription was allowed to proceed for the duration of the measurement phase, but cyclosporine A (CsA) was added to inactivate calcineurin directly after the priming phase, IFN-γ expression was reduced, but not abolished (Figure 4B). This indicates that nuclear NFAT continues to be transcriptionally active for some time after inactivation of calcineurin. Using a linear reference line (Figure 4C), we interpolated that gene expression during the NFAT memory phase quantitatively corresponded to what is achieved through 27.4 ± 0.8 (mean ± SEM, n = 3) minutes of continuous stimulation. Because stimulation with PMA+ionomycin is nonphysiological, we also performed this experiment with stimulation through peptide-pulsed splenocytes with similar results (Figures S4A–S4D).

Although treatment with CsA inhibits calcineurin-mediated activation of NFAT, it does not directly interrupt the other signaling pathways that are activated by PMA+ionomycin treatment or peptide-loaded APCs (Kiani et al., 2000) and therefore does not fully reflect the result of physical T cell-APC disengagement. To test more stringently whether NFAT memory can drive gene transcription in T cells under conditions that more closely mimic interruption of APC contact, we activated T cells with the lectin ConA and measured *Ifng* transcription after antagonization of ConA with α-MM (Das et al., 2009). In contrast to

Please cite this article in press as: Marangoni et al., The Transcription Factor NFAT Exhibits Signal Memory during Serial T Cell Interactions with Antigen-Presenting Cells, Immunity (2013), http://dx.doi.org/10.1016/j.immuni.2012.09.012

selective inhibition of NFAT activation, global interruption of ConA-induced TCR signaling did not allow for *Ifng* transcription during NFAT nuclear export (Figures 4D–4F).

In addition to NFAT, expression of IFN-γ also requires the transcription factor AP-1 (Macián et al., 2001), which is controlled by the Ras-ERK kinase pathway that may exhibit no or a much more transient memory activity than NFAT (Das et al., 2009; Faroudi et al., 2003). We therefore decided to examine whether AP-1-independent NFAT target genes may continue to be transcribed after interruption of ConA-induced TCR activation. The transcriptional regulator *Egr2* is one of the most rapidly expressed NFAT target genes that do not require AP-1 activity (Collins et al., 2008) and belongs to a group of so-called anergy-related genes because they are expressed in $CD4^+$ T cells treated with anergy-inducing regimens (Müller and Rao, 2010). Strikingly, expression of *Egr2* after α-MM-treatment was equivalent to its expression after CsA treatment, suggesting that NFAT can keep the *Egr2* locus transcriptionally active in the absence of other, more short-lived transcriptional activators required for IFN-γ-expression (Figures 4G and 4H; Figure S4E). We conclude from these observations that upon cessation of TCR signaling, NFAT continues to activate at least some, but not all of its target genes during delayed nuclear export, which may provide for a mechanism of differential NFAT-dependent gene expression during versus directly following APC interactions.

NFAT Activation in Motile Tumor-Infiltrating CTL

To explore the activation and deactivation kinetics of NFAT in a biologically relevant setting characterized by both stable and unstable T cell-APC contacts, we used MP-IVM and a modified dorsal skinfold chamber imaging technique to examine HA-CTL that migrate to and reject subcutaneously transplanted tumors (Figure 5A). Between 2 and 5 days after infusion into mice with established HA-expressing CT26 (CT26HA) tumors, HA-CTL that had initially entered through the stroma (data not shown) infiltrated the tumor parenchyma. Here they displayed heterogeneous migratory activity (Figure 5B; Movie S4), suggestive of both transient and more sustained interactions with tumor APCs, as previously described (Boissonnas et al., 2007; Mrass et al., 2006).

It is thought that TCR signaling in tumor-infiltrating T cells (TIL) is inefficient as a result of suboptimal Ag presentation (Spiotto et al., 2002), insufficient costimulation (Chen et al., 1992), dominant coinhibition (Dong et al., 2002), and various T cell intrinsic mechanisms that affect proximal TCR signal transduction (Frey and Monu, 2008). Thus, it could be expected that NFAT activation is less efficient in TIL. However, in cases where contact initiation of HA-CTL with HA-expressing tumor cells was observed, the kinetics of NFAT nuclear accumulation were similar to contacts with peptide-pulsed B cells, and CTL also decelerated and became, at least transiently, immobilized (Figure 5C; Movie S5). Unexpectedly, however, we found that NFAT was often partially or even fully nuclear in T cells that did not visibly engage with tumor cells and that were motile (Figures 5D–5F; Movie S6). Among HA-CTL with fully nuclear NFAT, 26% migrated faster than 4 μm/min, compared to 33% of cells with fully cytoplasmic NFAT. Conversely, 39% of CTL that moved slower than 4 μm/min showed no NFAT activation. Control experiments with tumors that lacked HA expression excluded NFAT activation due to Ag-independent Ca^{2+} transients (Revy et al., 2001) (Figures 5E and 5F; Movie S7). Hence, T cell arrest and NFAT activation were not strictly correlated, suggesting that either migratory T cells continue to sample TCR signals of sufficient strength to continuously induce NFAT activation, or that NFAT activation occurs during either stable or transient interactions, but is sustained independently of further TCR signals after APC disengagement and during subsequent motility, as observed for T_{CM}-B cell contacts in LNs.

NFAT Activation Occurs during Phases of Contact Stabilization

Even small Ca^{2+}-transients in naive T cells cause migratory pausing for at least several minutes in LNs (Wei et al., 2007) and, based on indirect comparisons between different in vitro studies, full NFAT activation requires higher cytosolic Ca^{2+} concentrations compared to cell immobilization (Bhakta et al., 2005; Dolmetsch et al., 1997; Negulescu et al., 1996). This suggests that NFAT activation only occurs during phases of at least transient immobilization. To directly test in which order HA-CTL immobilize and activate NFAT in response to increasing $[Ca^{2+}]_i$, we performed live-cell imaging experiments (Figure 6A). Thapsigargin (TG) induces an initial spike of high intracellular Ca^{2+}, followed within ~15 min by a stable plateau. Ca^{2+}-concentrations during this plateau phase can be controlled by increasing extracellular $[K^+]_e$, which depolarizes the plasma membrane and restricts cytosolic Ca^{2+}-influx (Negulescu et al., 1996). When we treated HA-CTL migrating on intercellular adhesion molecule-1 (ICAM-1)-coated plastic with TG under conditions of physiological $[K^+]_e$, they became uniformly immobilized and NFAT was fully nuclear during the plateau phase (Figures 6B–6D). In contrast, when $[Ca^{2+}]_i$ was kept at low but elevated concentrations compared to the resting state by raising extracellular $[K^+]_e$, some cells remained migratory, some immobilized with cytoplasmic NFAT, and some immobilized and had translocated NFAT to the nucleus in response to TG. However, we did not observe motile cells with fully nuclear NFAT, indicating that migratory arrest consistently preceded or paralleled NFAT nuclear accumulation. This makes it unlikely that HA-CTL in the tumor tissue sample TCR signals of sufficient strength to activate NFAT while actively migrating. Instead it suggests that nuclear NFAT in motile CTL in tumor tissue results from delayed export subsequent to NFAT activation during periods of immobilization through transient APC contacts.

CTL-Tumor Cell Contacts Are Destabilized during Treg Cell-Induced Tumor Tolerance

The observation that the effector cytokine gene *IFNg* is transcribed only during active TCR signaling, whereas the tolerance gene *Egr2* is transcribed also during the NFAT memory phase, prompted the hypothesis that under conditions of tolerance induction, T cells may form less stable contacts and disengage more frequently from APCs, therefore operate under NFAT memory more frequently and, through the resulting preferential expression of tolerance genes, lose their ability to reject tumors. Treg cells have been described to impair stable contact formation of effector T cells with DCs in LNs (Tadokoro et al., 2006; Tang et al., 2006) and also to promote tumor tolerance (Nishikawa and Sakaguchi, 2010). We therefore seeded animals

Please cite this article in press as: Marangoni et al., The Transcription Factor NFAT Exhibits Signal Memory during Serial T Cell Interactions with Antigen-Presenting Cells, Immunity (2013), http://dx.doi.org/10.1016/j.immuni.2012.09.012

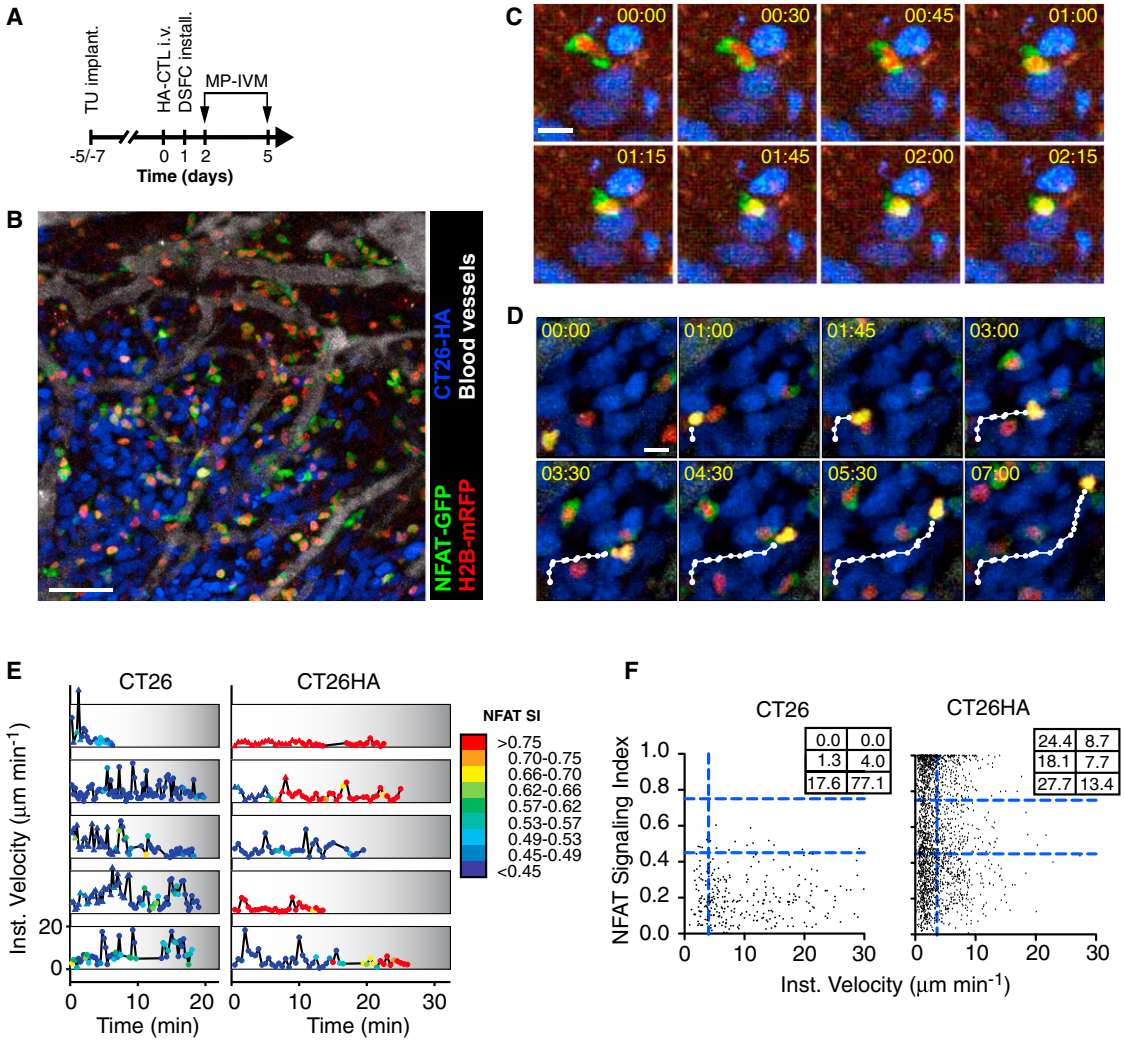

Figure 5. Rapid Activation and NFAT Memory in CTL during Tumor Rejection

(A) Experimental design.

(B) Intravital micrograph from the stroma-parenchyma border in a CT26HA tumor 5 days after injection of HA-CTL expressing NFAT-GFP (green) and H2B-mRFP (red). Tumor cells express H2B-Cerulean (blue). Blood plasma was visualized through i.v.-injected quantum dots (white). Scale bar represents 50 μm. See also Movies S4 and S6.

(C and D) Image sequences from similar recordings as shown in (B). (C) Rapid nuclear translocation of NFAT in an HA-CTL upon contact with an HA-expressing tumor cell. See also Movie S5. (D) Robust migration of an HA-CTL with nuclear NFAT. Time is in min:sec. Scale bar represents 10 μm in both (C) and (D).

(E) Correlation of NFAT activation (color-coded NFAT SI) and cell motility in CTL in the tumor parenchyma. Traces are selected from 269 (15 and 254 from CT26 and CT26HA tumors, respectively) recorded in two to eight movies per condition in two independent experiments.

(F) Population analysis of CTL instantaneous velocity and NFAT activation in the tumor parenchyma. Dot plots show data from one representative movie per condition, recorded 5 days after CTL transfer. Numbers in grids represent percentages in sectors.

with HA-specific Treg cells ("HA-Treg cells") (Klein et al., 2003) before tumor implantation (Figure 7A), which has previously been shown to allow effector differentiation in tumor-draining LNs but to abrogate tumor rejection by HA-specific CTL (Mempel et al., 2006). HA-Treg cells populated both tumor stroma and parenchyma and inhibited HA-CTL-mediated rejection of CT26HA tumors in skinfold chambers, indicating that they facilitated tumor tolerance (Figures S5A–S5C). Under these conditions we noted that when motile HA-CTL with cytoplasmic NFAT engaged with tumor cells, they typically responded with transient immobilization and NFAT activation that occurred with similar kinetics as in the absence of HA-Treg cells (Figure 7B; Movies S8 and S9; data not shown). Due to the high density of APCs in tumor tissue, even motile T cells were most of the time in close proximity to a tumor cell or presumably to other, nonvisualized, APCs capable of cross-presenting tumor Ag. It was therefore difficult to clearly identify events of full disengagement from APCs, and we could not determine the kinetics of NFAT export after unequivocal interruption of T cell-APC contact. Under the hypothesis that the rate of NFAT export might be changed in the presence of HA-Treg cells through the regulation of export kinases, we therefore analyzed the expression of

Please cite this article in press as: Marangoni et al., The Transcription Factor NFAT Exhibits Signal Memory during Serial T Cell Interactions with Antigen-Presenting Cells, Immunity (2013), http://dx.doi.org/10.1016/j.immuni.2012.09.012

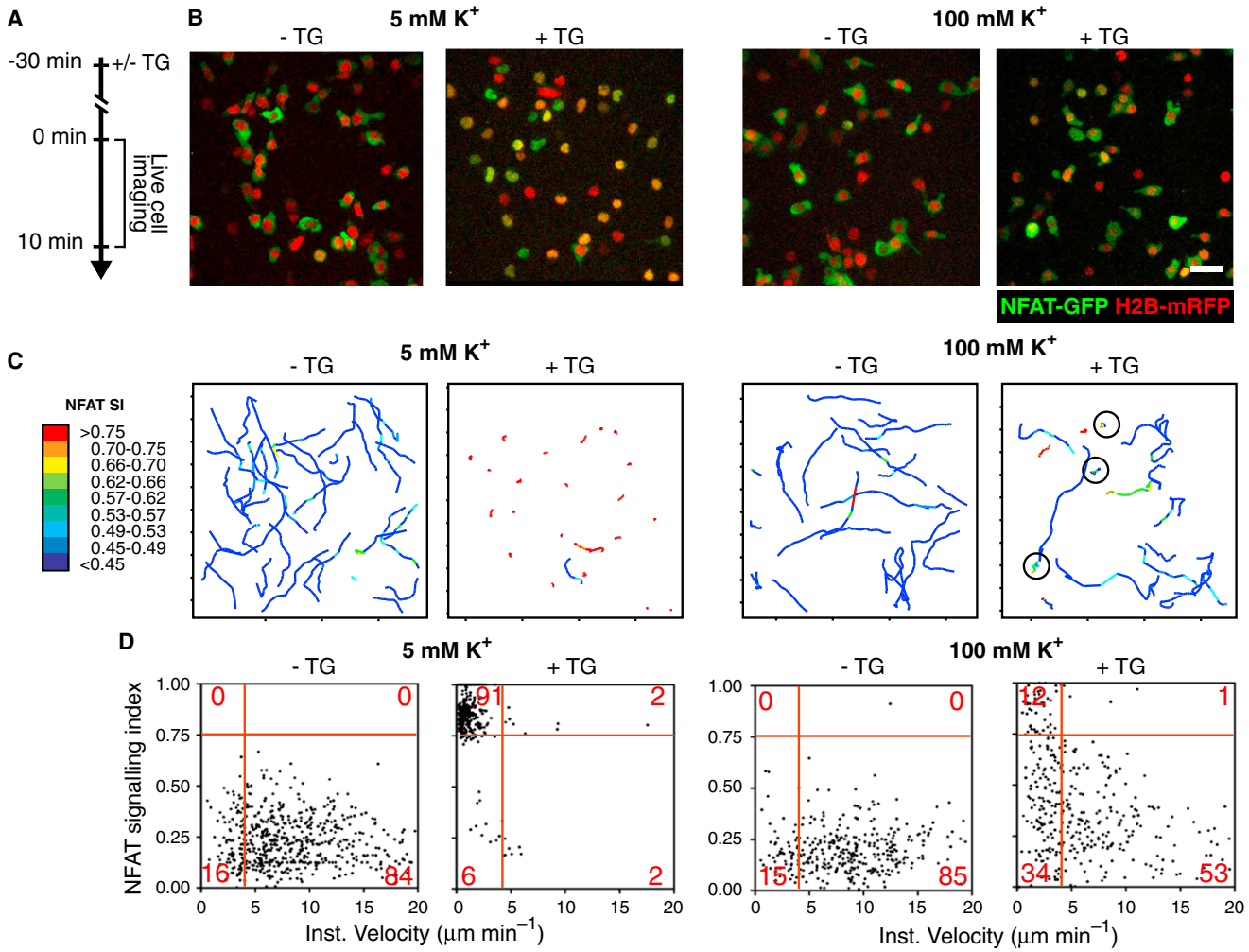

Figure 6. Rising Intracellular [Ca^{2+}] Leads to CTL Deceleration before Inducing NFAT Nuclear Translocation

(A) NFAT-GFP-expressing CTL were cultured in medium containing low (5 mM) or high (100 mM) concentrations of K^+ and treated (or not) with Thapsigargin (TG) for 30 min. Then, with TG present, their migration on ICAM-1-coated coverslips as well as NFAT activation was recorded for 10 min by live-cell imaging.

(B) Representative micrographs of all conditions tested.

(C) CTL migratory tracks. Color-code represents NFAT signaling index. Circles highlight tracks of immobilized CTL without NFAT activation.

(D) Correlation of cell motility and NFAT signaling index. One representative experiment out of two is shown.

members of all three know NFAT kinase families, as well as the phosphorylation of glycogen synthase kinase (GSK)-3β, which is reportedly regulated through the Akt kinase (Cross et al., 1995). However, we did not observe differences between tumor-infiltrating HA-CTL retrieved from mice seeded with HA-Treg cells or not (Figures S5D–S5F). Although there was thus no evidence that NFAT export kinetics were changed, we did observe that in tumors that were eventually rejected the frequency of motile cells among CTL with nuclear NFAT decreased over time (from 36.8% ± 9.8% on day 2 to 26.8% ± 4.3% at day 7 after transfer), while the frequency gradually increased in the presence of HA-Treg cells (from 34.3% ± 13.4% on day 2 to 42.2% ± 1.4% at day 7). This was reflected by more frequent and broader peaks of cell velocity with higher amplitude in the motility traces of HA-CTL with nuclear NFAT (Figure 7C). Tumor tolerance was therefore correlated with more widespread NFAT activity in motile CTL that had recently disengaged from a contact but had retained NFAT memory.

When HA-CTL coexpressed the unfused red fluorescent protein mCherry instead of H2B-mRFP, labeling of the cytoplasm in signaling cells revealed features characteristic of actively migrating cells, such as constant lamellipodial probing behavior at the leading edge (Figure 7B; Movie S9). This demonstrates that movement of CTL with nuclear NFAT is not passive and does not result from attachment to nonvisualized, migratory APCs, as observed for T cell-B cell contacts in LNs (Gunzer et al., 2004; Mempel et al., 2006; Okada et al., 2005).

NFAT Signaling in Motile CTL Is Increased during Treg Cell-Mediated Tumor Tolerance

During Treg cell-induced tolerance, CTL formed less stable contacts with APCs, but NFAT was often nuclear in individual

motile, tumor-infiltrating HA-CTL. This prompted us to examine how efficiently NFAT was activated in CTL on the population level during tumor immunity or tolerance. Interestingly, the frequency at which NFAT was fully nuclear (NFAT SI > 0.75) in CTL was fairly constant between two and seven days after their transfer into mice. Even more remarkably, the presence of HA-Treg cells that prevented tumor rejection did not lead to a decrease in NFAT activation in HA-CTL (Figure 7D).

To more directly relate the extent of NFAT activation to the stability of T cell-APC contacts, we analyzed the migratory arrest coefficient (AC), which is a commonly used measure of T cell contact stabilization, in individual CTL specifically during phases of sustained NFAT nuclear translocation. We found that HA-Treg cells caused a progressive uncoupling of NFAT activation and the formation of stable contacts, so that nearly 80% of CTL with nuclear NFAT were motile (AC < 0.7) 1 week after transfer into tumor-bearing mice harboring HA-Treg cells, compared to 30% motile cells in their absence (Figures 7E and 7F).

Our data suggest that total NFAT activation is comparable during tumor rejection and development of tumor tolerance, which is characterized by unstable T cell-APC interactions and enhanced CTL migratory activity. Based on the idea that NFAT signaling in motile cells favors the induction of tolerance through preferential expression of *Egr2* and related genes during the NFAT memory phase, we wanted to develop a parameter that quantified the degree of NFAT activity in motile CTL. To this end, we calculated the "NFAT signaling × motility index," which is essentially a measure of cumulative NFAT signaling activity occurring during phases of migratory activity in a population of T cells, normalized to the cumulative cell observation time (Figure S5G). This analysis indicated that the amount of NFAT signaling that occurs in motile cells indeed rose with decreasing APC contact stability and was increased by more than 7-fold when HA-Treg cell-induced contact destabilization was maximal (Figure 7G). Therefore, although we could not determine whether NFAT export kinetics were altered under the influence of Treg cells, the development of tolerance was paralleled by a pronounced shift away from NFAT signaling during stable T cell-APC contacts and toward NFAT signaling in motile cells outside of APC contacts, which was facilitated by NFAT signal memory.

In summary, we present here an MP-IVM-based approach to examine directly in vivo the activation of transcriptional responses through dynamic cellular interactions in the immune system. This approach adds an additional dimension to our ability to dissect the events that determine the outcome of immune responses as they occur in their full complexity in vivo. We report that the transcription factor NFAT remains transcriptionally active during its delayed export from the nucleus after disengagement of T cells from APCs. However, only some NFAT target genes are expressed during this NFAT memory phase, but not others, suggesting a mechanism by which variations in the dynamics of cell-cell interactions in the immune system can be translated into different gene expression programs.

DISCUSSION

T cells at various stages of development are programmed to continually migrate through either lymphoid or nonlymphoid tissues and sample and decode immunologically-relevant information provided by APCs. By flexibly translating the multitude of signals they collect into different transcriptional programs, they are able to respond appropriately through tolerance or through induction and execution of their various effector functions. Here we have developed an MP-IVM approach to investigate the sensitivity and the kinetics with which individual T cells respond in vivo to encounters with their cognate Ag by activating and translocating the canonical transcription factor NFAT from the cytoplasm to the nucleus. We found that contacts both to B cells pulsed with high doses of antigenic peptide as well as to tumor cells, presumably presenting Ag suboptimally, rapidly induced maximal nuclear accumulation of NFAT in Ag-experienced $CD8^+$ T cells. Contacts with B cells were mostly stable, but upon contact dissolution, NFAT nuclear export was 20 times slower than import, irrespective of the duration of an individual contact. During delayed nuclear export, NFAT remained transcriptionally active for the tolerance-associated gene *Egr2*, but not for the effector gene *Ifng*. Under conditions of Treg cell-mediated tumor tolerance, where CTL-APC contacts in tumors were destabilized, we observed that fast import and delayed nuclear export kinetics enabled T cells to continuously retain NFAT in the nucleus during and in between serial, transient APC interactions. As a consequence, NFAT activation was similar in tumor-infiltrating CTL, irrespective of the stability of APC contacts or the final biological outcome.

Over the past decade, dynamic imaging of the immune system in the context of intact tissues has highlighted the mobility of T cells and other immune cells and how flexibly they form and dissolve both stable and unstable contacts with multiple, changing partners. What is not known is the sensitivity with which the gene regulatory mechanisms that control cellular differentiation respond to the constantly changing external cues T cells receive. Here we show that nuclear accumulation of NFAT, a key transcriptional regulator in T cells, is uniform in response to Ag presented optimally or suboptimally to Ag-experienced $CD8^+$ T cells. In each case nuclear import occurred with only minimal delay upon APC contact and consistently reached maximal values. The molecular basis for the apparently digital nature of this response may reside in the cooperativity of multiple dephosphorylation events that control nuclear import (Podtschaske et al., 2007). Based on these observations, neither the speed nor the extent of NFAT nuclear accumulation strictly reflects the quality of the Ag receptor stimulus, as determined by the avidity of pMHC-TCR interactions or the amount of costimulation.

A TCR-dependent increase in cytosolic Ca^{2+} is not only essential for NFAT activation but also both sufficient and required for immobilization of T cells (Bhakta et al., 2005; Dustin et al., 1997; Negulescu et al., 1996; Wei et al., 2007). By live-cell imaging at increasing $[Ca^{2+}]_i$ we found that NFAT activation did not occur without prior, at least partial, CTL immobilization. This could reflect a need for at least transient stabilization of APC contacts in order to sustain a Ca^{2+}-signal sufficient for NFAT activation. Alternatively, these two events may simply coincide without being interdependent, and the order in which they occur merely reflects a slightly higher Ca^{2+}-sensitivity of cell arrest compared to NFAT activation. In contrast to fast import, nuclear export of NFAT upon disengagement from

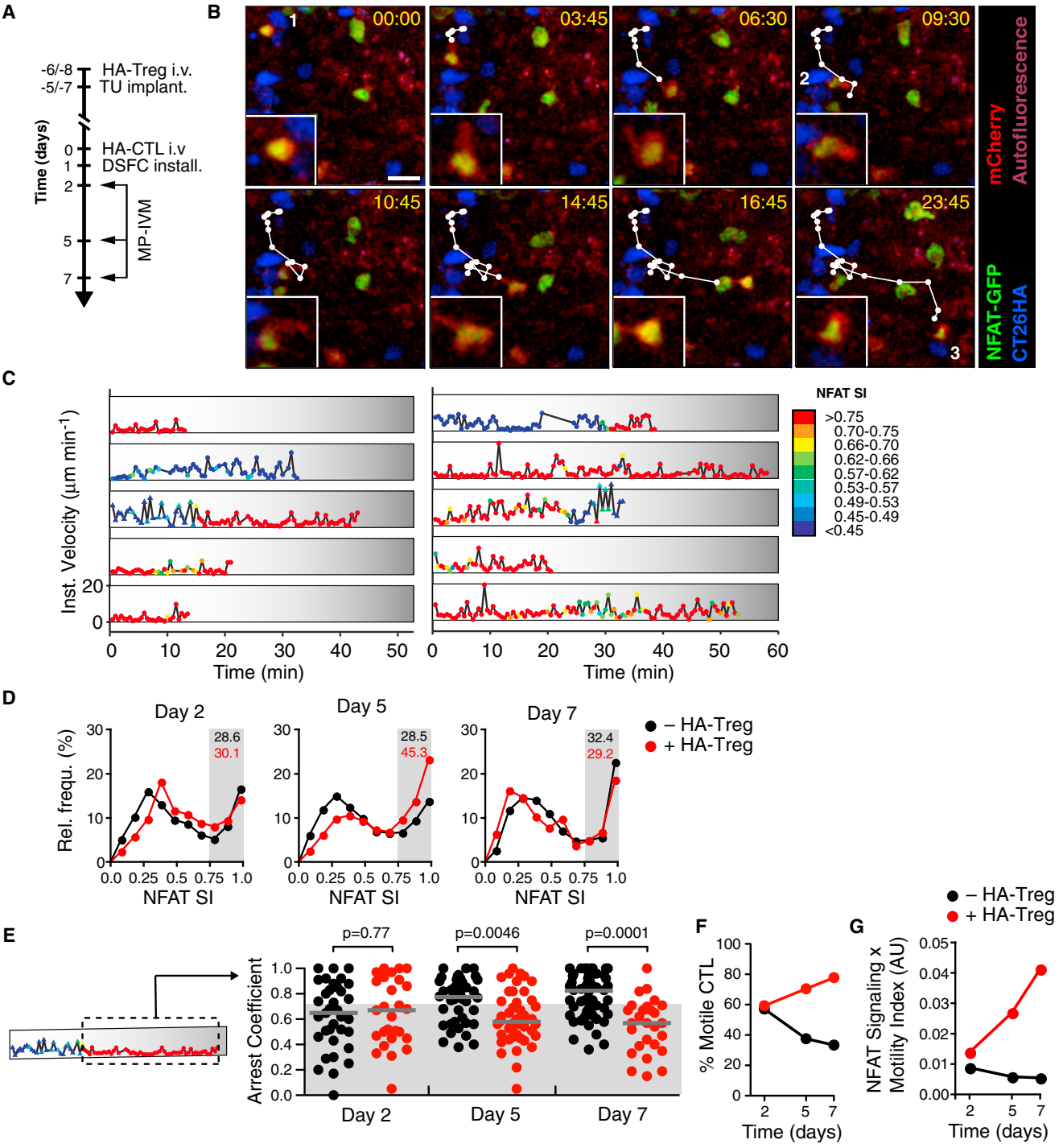

Figure 7. Comparable NFAT Activation through Stable and Unstable CTL-APC Contacts in Tumor Tissue

(A) Experimental design: Prior to tumor implantation, mice were seeded with HA-Treg cells.

(B) Image sequence showing HA-CTL expressing NFAT-GFP (green) and mCherry (red) sequentially interacting with at least three different tumor cells (marked 1, 2, 3). Note that NFAT stays nuclear between cell contacts, evident in insets showing magnified views of the CTL. See also Movie S9. Time in min:sec. Scale bar represents 20 μm.

(C) Correlation of NFAT activation (color-coded NFAT SI) and motility in HA-CTL in the tumor parenchyma in presence or absence of HA-Treg cells. Traces are selected from 420 (254 and 166 in absence and presence of HA-Treg cells, respectively) recorded in eight to nine movies per condition, from two independent experiments.

(D) Distribution of instantaneous NFAT activation states in HA-CTL infiltrating the tumor parenchyma in presence (red lines) or absence (black lines) of HA-Treg cells at the indicated time-points after CTL transfer. Numbers indicate percentage of events with NFAT SI > 0.75. Data are pooled for each time point and condition.

(legend continued on next page)

Ag-presenting B cells in the LN was significantly slower, with a typical half-life of nuclear NFAT of 20 min. These export kinetics were independent of ongoing calcineurin-mediated NFAT activation but primarily determined by the activity of NFAT export kinases GSK-3, CK1, and DYRK1 (Müller and Rao, 2010), with CK1 having the quantitatively largest contribution. Because of the high APC density in tumors, we could not follow individual CTL for long enough after disengagement from one and before encounter of the next APC in order to examine potential changes to the NFAT nuclear export rate under the influence of Treg cells. Therefore, although we did not see altered expression or activity of NFAT kinases in tumor-infiltrating CTL during tolerance, we cannot strictly exclude changes in NFAT export rate through other mechanisms.

It must be noted that our studies focused on NFAT1, and it will be interesting to examine the behavior of NFAT 2 and 4, whose activation may require different Ca^{2+} concentrations than NFAT1 (Srinivasan and Frauwirth, 2007), and which may vary in their use of available export mechanisms (Hogan et al., 2003).

Previous work has demonstrated that transcriptional activity in effector T cells, at least of cytokine genes, is tightly regulated through Ag receptor signals (Slifka et al., 1999), which at the same time control both directional and nondirectional cytokine secretion (Kupfer et al., 1991). It was therefore surprising to observe at least transient NFAT-dependent transcriptional activity of the *Ifng* locus after inactivation of calcineurin, which indicates that NFAT remains bound to gene-regulatory sequences for some time following the interruption of an NFAT activating stimulus. However, experiments where the consequences of T cell-APC contact dissolution were more closely mimicked by interruption of TCR triggering, and where *Ifng* was not transcribed during the NFAT memory phase, further supported the notion that not only the secretion but also the expression of this cytokine is tightly linked to APC interactions. This may be because the activity of signaling pathways regulating other transcriptional activators necessary to transcribe *Ifng*, such as Ras and ERK activating AP-1, exhibit a shorter signal memory (Das et al., 2009; Faroudi et al., 2003). Expression of *Egr2*, on the other hand, which does not require AP-1 (Collins et al., 2008), was prolonged into the signal memory phase. This is reminiscent of the well-established observation that NFAT activation can have different functional outcomes depending on its cooperation with other transcription factors. NFAT dimers induce the transcription of genes involved in T cell tolerance (Soto-Nieves et al., 2009), whereas NFAT interaction with other DNA-binding factors that require stronger TCR signals or costimulation, such as AP-1, facilitates activation of effector programs of immunity (Macian, 2005).

One traditionally held view is that differential activation of NFAT and its transcriptional partners at the very onset of a T cell-APC encounter, based on the strength of the TCR signal and on costimulation, determine the transcriptional response of the T cell. Our observations do not disprove this hypothesis but raise the alternative, and not mutually exclusive possibility, that signal quality and strength determine the ability of T cells to form stable, long-lasting contacts and that the stability of the contacts, in turn, has important consequences for the transcriptional outcome. For one, stable contacts may be required for T cells to receive instructive signals in the form of cytokines secreted into the immune synapse by the APC (Pulecio et al., 2010). Second, as shown here, less stable contacts and more frequent APC disengagement will increase the relative amount of time a T cell spends in NFAT memory during its migration between APC encounters relative to the time it spends in direct APC contact. Based on our observations on transcription in the NFAT memory phase, the balance of APC contact time and NFAT memory time could determine the extent to which NFAT can cooperate with its different transcriptional partners and ultimately, the induction of immunity or tolerance. In line with this hypothesis, ex vivo analysis of tumor-infiltrating HA-CTL demonstrated lower expression of the NFAT-dependent effector genes *Ifng* and *Tnfa* in mice injected with HA-Treg cells, whereas expression of the NFAT-dependent, tolerance-associated PD-1 gene *Pdcd1* was increased (C.A. Bauer, E.Y.K, and T.R.M, data not shown). Interestingly, T cells primed by ICAM-1-deficient DCs that are unable to support stable T cell contacts respond by apparently normal initial activation but then produce much lower amounts of IFN-γ and are eventually deleted (Scholer et al., 2008).

Further insights into how T cell differentiation and effector functions are dynamically regulated through APC interactions will likely come from studies in which NFAT activation is monitored together with pathways activating other gene regulatory factors that cooperate with NFAT to activate the genetic programs they specify.

In conclusion, we show that T cells respond near-instantaneously to physiological APC contacts in vivo through activation and nuclear localization of NFAT but upon disengagement from APCs deactivate this transcription factor with delayed kinetics. This short-term biochemical imprint of recent APC encounters facilitates expression of the tolerance factor *Egr2*, but not of the immunity gene *Ifng*. We propose that under conditions that lead to unstable APC contacts, NFAT activation in T cells is not impaired, but diverted into a tolerogenic program, possibly through increased transcription of tolerance genes during NFAT memory.

EXPERIMENTAL PROCEDURES

Live-Cell Imaging of CTL Motility and NFAT-GFP Nucleocytoplasmic Shuttling

To examine CTL motility and NFAT activation at varying $[Ca^{2+}]_i$, HA-CTL were transferred into medium with either low (5 mM) or high (100 mM) K^+ concentration and allowed to adhere to murine ICAM-1-Fc-coated (12.5 μg/ml, R&D Systems) plastic. High $[K^+]_e$ depolarizes the cell membrane

(E) Arrest coefficient (AC) analysis of CTL track segments defined by continuous NFAT activation (SI > 0.75 for > 2 min) at the indicated time points in absence (back symbols) or presence (red symbols) of HA-Treg cells. Each symbol represents an individual track segment, bars represent medians. The shaded area highlights data points representing nonarrested cells (AC < 0.7). P values were determined by Mann-Whitney test. Pooled data represent all "$NFAT_{on}$ segments" in two to three movies per condition and time point, collected in two independent experiments.

(F) Graphic summary of data in (E).

(G) NFAT Signaling x Motility Index analysis in HA-CTL infiltrating the tumor parenchyma.

and reduces the driving force for cytosolic Ca^{2+}-influx upon cell activation. Cells were either left untreated or activated with 2 μM thapsigargin, cultured for 30 min to allow for stabilization of $[Ca^{2+}]_i$ at different concentrations and then recorded by multiphoton live-cell imaging for 10 min at 30 s intervals.

Calculation of NFAT Memory Time

HA-CTL were prestimulated for 30 min with 1 μg/ml ionomycin and 50 ng/ml PMA or with splenocytes pulsed with 10^{-9} M $HA_{515-523}$ peptide (1:4 ratio). Alternatively, cells were prestimulated with concanavalin A (10 μg/ml) for 15 min. Subsequent stimulation was carried out for 60 min in presence of BFA, along with 100 μg/ml cycloheximide (CHX), 1 μM CsA, 100 mM αMM, or 50 μg/ml ActD. ActD was added 15, 30, 45, or 60 min after BFA. Cells were then stained for intracellular IFN-γ and Egr2 and analyzed by flow cytometry.

MP-IVM Recordings of T_{CM} and CTL in LNs and Tumors

All experiments were in accordance with NIH guidelines and were approved by the Institutional Animal Committees of Massachusetts General Hospital. Analysis of T-B cell interactions in LNs was carried out as previously described (Mempel et al., 2006).

Dorsal skinfold chamber (DSFC) tumors were grown with modifications from previously published techniques (Fukumura et al., 1998). Two aliquots of 10^6 H2B-Cerulean-expressing tumor cells were subcutaneously injected in the backs of mice, the first proximal to the neck (to ensure continued robust lymphatic drainage of tumor tissue after installation of DSFCs over the second tumor), the second ~1.5 cm left of the dorsal midline approximately halfway from the neck to the tail base. Five to seven days later, 5×10^6 NFAT-GFP- and H2B-mRFP-expressing HA-CTL were injected i.v. The following day, DSFCs were installed in a way that the distal tumor was centered in the imaging chamber and accessible to longitudinal investigation by MP-IVM, which was performed under general anesthesia with Ketamine and Xylazine on days 2, 5, and 7 after CTL transfer. Blood plasma was visualized by i.v. injection of 2 μl (4 pmol) of QTracker 655 quantum dot suspension (Invitrogen).

Some mice were injected i.v. with 10^6 $CD4^+$ $CD25^+$ HA-Treg cells purified from pgk-HAxTCR-HA mice by immunomagnetic selection (Miltenyi Biotech) 1 day before tumor implantation.

Analysis of NFAT Nucleocytoplasmic Shuttling

The spatial overlap between NFAT-GFP and H2B-mRFP signals was used to calculate the NFAT SI as a measure of NFAT nuclear accumulation (see also Figure S2). To this end, centroids of H2B-mRFP-stained cell nuclei were measured in Imaris (Bitplane) and used to define the nuclear center. Normalized 2D-radial profile integrated fluorescence intensity histograms were then generated for EGFP and mRFP signals, using ImageJ and the radial profile plug-in (http://rsbweb.nih.gov/ij/plugins/radial-profile.html), to assess the distribution of each reporter as a function of distance from nuclear centers. In individual recordings, we found that in nonsignaling cells with visually determined nuclear exclusion of NFAT-GFP, this overlap was 30%–40% (due to deviation from perfect sphericity of most nuclei as well as the 3D geometry of cells), whereas full nuclear accumulation yielded 100% overlap. To adjust for slight variability between different experiments, we arbitrarily defined an SI of 0 to represent the first percentile of the distribution of overlap values obtained from an individual recording, whereas 100% overlap was defined as an SI of 1. All annotation of NFAT signaling status was automated through ImageJ scripting and validated visually.

Statistical Analysis

For normally distributed data, experimental groups were compared through Student's t test. Otherwise, Mann-Whitney test was used.

SUPPLEMENTAL INFORMATION

Supplemental Information includes five figures, Supplemental Experimental Procedures, and nine videos and can be found with this article online at http://dx.doi.org/10.1016/j.immuni.2012.09.012.

ACKNOWLEDGMENTS

We thank Jose Aramburu, Ulrich von Andrian, Shiv Pillai, James Moon, and Anjana Rao for helpful suggestions and critical reading of the manuscript, as well as Harald von Boehmer, Jose Aramburu, Vigo Heissmeyer, Roberto Bonasio, Sean Megason, Paul Allen, and Jason McCarthy for providing key reagents. We are indebted to Julia Kahn from the laboratory of Dai Fukumura for technical advice. T.R.M. was supported by NIH grants AI073457, CA150975, AI0178897, and AI097052 as well as a grant by the Dana Foundation. F.M. was supported by an MGH Fund for Medical Discovery Fellowship. T.T.M. was supported by the MGH ECOR Tosteson Postdoctoral Fellowship Award.

Received: March 20, 2012
Accepted: September 27, 2012
Published: January 10, 2013

REFERENCES

Aramburu, J., Yaffe, M.B., López-Rodríguez, C., Cantley, L.C., Hogan, P.G., and Rao, A. (1999). Affinity-driven peptide selection of an NFAT inhibitor more selective than cyclosporin A. Science *285*, 2129–2133.

Bhakta, N.R., Oh, D.Y., and Lewis, R.S. (2005). Calcium oscillations regulate thymocyte motility during positive selection in the three-dimensional thymic environment. Nat. Immunol. *6*, 143–151.

Boissonnas, A., Fetler, L., Zeelenberg, I.S., Hugues, S., and Amigorena, S. (2007). In vivo imaging of cytotoxic T cell infiltration and elimination of a solid tumor. J. Exp. Med. *204*, 345–356.

Bromley, S.K., Peterson, D.A., Gunn, M.D., and Dustin, M.L. (2000). Cutting edge: hierarchy of chemokine receptor and TCR signals regulating T cell migration and proliferation. J. Immunol. *165*, 15–19.

Celli, S., Garcia, Z., and Bousso, P. (2005). CD4 T cells integrate signals delivered during successive DC encounters in vivo. J. Exp. Med. *202*, 1271–1278.

Chen, L., Ashe, S., Brady, W.A., Hellström, I., Hellström, K.E., Ledbetter, J.A., McGowan, P., and Linsley, P.S. (1992). Costimulation of antitumor immunity by the B7 counterreceptor for the T lymphocyte molecules CD28 and CTLA-4. Cell *71*, 1093–1102.

Clark, C.E., Hasan, M., and Bousso, P. (2011). A role for the immediate early gene product c-fos in imprinting T cells with short-term memory for signal summation. PLoS ONE *6*, e18916.

Collins, S., Lutz, M.A., Zarek, P.E., Anders, R.A., Kersh, G.J., and Powell, J.D. (2008). Opposing regulation of T cell function by Egr-1/NAB2 and Egr-2/Egr-3. Eur. J. Immunol. *38*, 528–536.

Cross, D.A., Alessi, D.R., Cohen, P., Andjelkovich, M., and Hemmings, B.A. (1995). Inhibition of glycogen synthase kinase-3 by insulin mediated by protein kinase B. Nature *378*, 785–789.

Das, J., Ho, M., Zikherman, J., Govern, C., Yang, M., Weiss, A., Chakraborty, A.K., and Roose, J.P. (2009). Digital signaling and hysteresis characterize ras activation in lymphoid cells. Cell *136*, 337–351.

Dolmetsch, R.E., Lewis, R.S., Goodnow, C.C., and Healy, J.I. (1997). Differential activation of transcription factors induced by Ca2+ response amplitude and duration. Nature *386*, 855–858.

Dong, H., Strome, S.E., Salomao, D.R., Tamura, H., Hirano, F., Flies, D.B., Roche, P.C., Lu, J., Zhu, G., Tamada, K., et al. (2002). Tumor-associated B7-H1 promotes T-cell apoptosis: a potential mechanism of immune evasion. Nat. Med. *8*, 793–800.

Dustin, M.L., Bromley, S.K., Kan, Z., Peterson, D.A., and Unanue, E.R. (1997). Antigen receptor engagement delivers a stop signal to migrating T lymphocytes. Proc. Natl. Acad. Sci. USA *94*, 3909–3913.

Faroudi, M., Zaru, R., Paulet, P., Müller, S., and Valitutti, S. (2003). Cutting edge: T lymphocyte activation by repeated immunological synapse formation and intermittent signaling. J. Immunol. *171*, 1128–1132.

Fife, B.T., Pauken, K.E., Eagar, T.N., Obu, T., Wu, J., Tang, Q., Azuma, M., Krummel, M.F., and Bluestone, J.A. (2009). Interactions between PD-1 and

PD-L1 promote tolerance by blocking the TCR-induced stop signal. Nat. Immunol. *10*, 1185–1192.

Frey, A.B., and Monu, N. (2008). Signaling defects in anti-tumor T cells. Immunol. Rev. *222*, 192–205.

Fukumura, D., Xavier, R., Sugiura, T., Chen, Y., Park, E.C., Lu, N., Selig, M., Nielsen, G., Taksir, T., Jain, R.K., and Seed, B. (1998). Tumor induction of VEGF promoter activity in stromal cells. Cell *94*, 715–725.

Germain, R.N., Bajénoff, M., Castellino, F., Chieppa, M., Egen, J.G., Huang, A.Y., Ishii, M., Koo, L.Y., and Qi, H. (2008). Making friends in out-of-the-way places: how cells of the immune system get together and how they conduct their business as revealed by intravital imaging. Immunol. Rev. *221*, 163–181.

Gunzer, M., Weishaupt, C., Hillmer, A., Basoglu, Y., Friedl, P., Dittmar, K.E., Kolanus, W., Varga, G., and Grabbe, S. (2004). A spectrum of biophysical interaction modes between T cells and different antigen-presenting cells during priming in 3-D collagen and in vivo. Blood *104*, 2801–2809.

Henrickson, S.E., Mempel, T.R., Mazo, I.B., Liu, B., Artyomov, M.N., Zheng, H., Peixoto, A., Flynn, M.P., Senman, B., Junt, T., et al. (2008). T cell sensing of antigen dose governs interactive behavior with dendritic cells and sets a threshold for T cell activation. Nat. Immunol. *9*, 282–291.

Hogan, P.G., Chen, L., Nardone, J., and Rao, A. (2003). Transcriptional regulation by calcium, calcineurin, and NFAT. Genes Dev. *17*, 2205–2232.

Kiani, A., Rao, A., and Aramburu, J. (2000). Manipulating immune responses with immunosuppressive agents that target NFAT. Immunity *12*, 359–372.

Klein, L., Khazaie, K., and von Boehmer, H. (2003). In vivo dynamics of antigen-specific regulatory T cells not predicted from behavior in vitro. Proc. Natl. Acad. Sci. USA *100*, 8886–8891.

Kupfer, A., Mosmann, T.R., and Kupfer, H. (1991). Polarized expression of cytokines in cell conjugates of helper T cells and splenic B cells. Proc. Natl. Acad. Sci. USA *88*, 775–779.

Macian, F. (2005). NFAT proteins: key regulators of T-cell development and function. Nat. Rev. Immunol. *5*, 472–484.

Macián, F., López-Rodríguez, C., and Rao, A. (2001). Partners in transcription: NFAT and AP-1. Oncogene *20*, 2476–2489.

Mempel, T.R., Henrickson, S.E., and Von Andrian, U.H. (2004). T-cell priming by dendritic cells in lymph nodes occurs in three distinct phases. Nature *427*, 154–159.

Mempel, T.R., Pittet, M.J., Khazaie, K., Weninger, W., Weissleder, R., von Boehmer, H., and von Andrian, U.H. (2006). Regulatory T cells reversibly suppress cytotoxic T cell function independent of effector differentiation. Immunity *25*, 129–141.

Miller, M.J., Safrina, O., Parker, I., and Cahalan, M.D. (2004). Imaging the single cell dynamics of CD4+ T cell activation by dendritic cells in lymph nodes. J. Exp. Med. *200*, 847–856.

Mrass, P., Takano, H., Ng, L.G., Daxini, S., Lasaro, M.O., Iparraguirre, A., Cavanagh, L.L., von Andrian, U.H., Ertl, H.C., Haydon, P.G., and Weninger, W. (2006). Random migration precedes stable target cell interactions of tumor-infiltrating T cells. J. Exp. Med. *203*, 2749–2761.

Müller, M.R., and Rao, A. (2010). NFAT, immunity and cancer: a transcription factor comes of age. Nat. Rev. Immunol. *10*, 645–656.

Negulescu, P.A., Krasieva, T.B., Khan, A., Kerschbaum, H.H., and Cahalan, M.D. (1996). Polarity of T cell shape, motility, and sensitivity to antigen. Immunity *4*, 421–430.

Nishikawa, H., and Sakaguchi, S. (2010). Regulatory T cells in tumor immunity. Int. J. Cancer *127*, 759–767.

Okada, T., Miller, M.J., Parker, I., Krummel, M.F., Neighbors, M., Hartley, S.B., O'Garra, A., Cahalan, M.D., and Cyster, J.G. (2005). Antigen-engaged B cells undergo chemotaxis toward the T zone and form motile conjugates with helper T cells. PLoS Biol. *3*, e150.

Pittet, M.J., and Mempel, T.R. (2008). Regulation of T-cell migration and effector functions: insights from in vivo imaging studies. Immunol. Rev. *221*, 107–129.

Podtschaske, M., Benary, U., Zwinger, S., Höfer, T., Radbruch, A., and Baumgrass, R. (2007). Digital NFATc2 activation per cell transforms graded T cell receptor activation into an all-or-none IL-2 expression. PLoS ONE *2*, e935.

Pulecio, J., Petrovic, J., Prete, F., Chiaruttini, G., Lennon-Dumenil, A.M., Desdouets, C., Gasman, S., Burrone, O.R., and Benvenuti, F. (2010). Cdc42-mediated MTOC polarization in dendritic cells controls targeted delivery of cytokines at the immune synapse. J. Exp. Med. *207*, 2719–2732.

Qureshi, O.S., Zheng, Y., Nakamura, K., Attridge, K., Manzotti, C., Schmidt, E.M., Baker, J., Jeffery, L.E., Kaur, S., Briggs, Z., et al. (2011). Trans-endocytosis of CD80 and CD86: a molecular basis for the cell-extrinsic function of CTLA-4. Science *332*, 600–603.

Revy, P., Sospedra, M., Barbour, B., and Trautmann, A. (2001). Functional antigen-independent synapses formed between T cells and dendritic cells. Nat. Immunol. *2*, 925–931.

Scholer, A., Hugues, S., Boissonnas, A., Fetler, L., and Amigorena, S. (2008). Intercellular adhesion molecule-1-dependent stable interactions between T cells and dendritic cells determine CD8+ T cell memory. Immunity *28*, 258–270.

Skokos, D., Shakhar, G., Varma, R., Waite, J.C., Cameron, T.O., Lindquist, R.L., Schwickert, T., Nussenzweig, M.C., and Dustin, M.L. (2007). Peptide-MHC potency governs dynamic interactions between T cells and dendritic cells in lymph nodes. Nat. Immunol. *8*, 835–844.

Slifka, M.K., Rodriguez, F., and Whitton, J.L. (1999). Rapid on/off cycling of cytokine production by virus-specific CD8+ T cells. Nature *401*, 76–79.

Soto-Nieves, N., Puga, I., Abe, B.T., Bandyopadhyay, S., Baine, I., Rao, A., and Macian, F. (2009). Transcriptional complexes formed by NFAT dimers regulate the induction of T cell tolerance. J. Exp. Med. *206*, 867–876.

Spiotto, M.T., Yu, P., Rowley, D.A., Nishimura, M.I., Meredith, S.C., Gajewski, T.F., Fu, Y.X., and Schreiber, H. (2002). Increasing tumor antigen expression overcomes "ignorance" to solid tumors via crosspresentation by bone marrow-derived stromal cells. Immunity *17*, 737–747.

Srinivasan, M., and Frauwirth, K.A. (2007). Reciprocal NFAT1 and NFAT2 nuclear localization in CD8+ anergic T cells is regulated by suboptimal calcium signaling. J. Immunol. *179*, 3734–3741.

Stinchcombe, J.C., Bossi, G., Booth, S., and Griffiths, G.M. (2001). The immunological synapse of CTL contains a secretory domain and membrane bridges. Immunity *15*, 751–761.

Tadokoro, C.E., Shakhar, G., Shen, S., Ding, Y., Lino, A.C., Maraver, A., Lafaille, J.J., and Dustin, M.L. (2006). Regulatory T cells inhibit stable contacts between CD4+ T cells and dendritic cells in vivo. J. Exp. Med. *203*, 505–511.

Tang, Q., Adams, J.Y., Tooley, A.J., Bi, M., Fife, B.T., Serra, P., Santamaria, P., Locksley, R.M., Krummel, M.F., and Bluestone, J.A. (2006). Visualizing regulatory T cell control of autoimmune responses in nonobese diabetic mice. Nat. Immunol. *7*, 83–92.

Tomida, T., Hirose, K., Takizawa, A., Shibasaki, F., and Iino, M. (2003). NFAT functions as a working memory of Ca2+ signals in decoding Ca2+ oscillation. EMBO J. *22*, 3825–3832.

Wei, S.H., Safrina, O., Yu, Y., Garrod, K.R., Cahalan, M.D., and Parker, I. (2007). Ca2+ signals in CD4+ T cells during early contacts with antigen-bearing dendritic cells in lymph node. J. Immunol. *179*, 1586–1594.